

SPbU-IP-00-06

Nucleus-nucleus scattering in perturbative QCD with $N_c \rightarrow \infty$

M.Braun

Department of High Energy physics, University of S.Petersburg,
198904 S.Petersburg, Russia

October 23, 2018

Abstract. In the perturbative QCD with $N_c \rightarrow \infty$ equations for the amplitude of the nucleus-nucleus scattering are derived by the effective field method. The asymptotic form of the solution is discussed. It is argued that in the high-energy limit the total nucleus-nucleus cross-sections become constant and purely geometrical.

1 Introduction

In the framework of the colour dipole model of A.H.Mueller [1,2] it follows that in the high-colour limit $N_c \rightarrow \infty$ the scattering on a heavy nucleus is exactly described by the sum of fan diagrams constructed of BFKL pomerons, each of them splitting into two [3]. The equation for the sum of BFKL fan diagrams was first written by I.Balitsky [4] in his original operator expansion formalism. Then it was rederived by Yu.Kovchegov [5] in the colour dipole framework and by the author by directly summing the BFKL fan diagrams [6]. The perturbative solution of this equation in the region of small non-linearity (outside the saturation region) was studied in [7]. Asymptotic estimates of the solution were presented in [8]. Finally in [6] the exact solution of the equation was obtained by direct numerical methods. The main physical results following from these studies are that, first, at high rapidities Y the hA total cross-section saturates to its geometrical limit $2\pi R_A^2$ and, second, the gluon density in the nucleus acquires a form of a soliton in $Y - \ln k$ space moving towards higher momenta with nearly a constant velocity as Y increases. This last property supports the applicability of the perturbative treatment, since the well-know diffusion of the BFKL pomeron towards small momenta results to be stopped.

In the present paper we attempt to generalize these results to nucleus-nucleus (AB) scattering. In this case, in the $N_c \rightarrow \infty$ limit the total amplitude is given by the sum of all tree diagrams constructed of BFKL pomerons and the triple pomeron vertex. In contrast to the hA case, the vertex now describes not only splitting of a pomeron into two but also fusion of two pomerons into one. The diagrams for the amplitude accordingly result much more complicated than the fan diagrams relevant for the hA case. However, using the effective field theory methods developed for summing such diagrams long ago [9,10], one can construct an equation which describes the AB amplitude. Naturally this equation (in fact a pair of equations) results much more complicated than for the case of hA scattering. Its exact (numerical) solution does not seem realistic. However simple asymptotic estimates, analogous to the ones

made in [7,8], show that the total AB cross-section tends to its geometrical limit at high rapidities similar to the hA case.

Unfortunately the gluon density in the overlapping area cannot be found from these estimates, but rather requires knowledge of the solution in more detail. We leave this problem for future studies.

2 Effective field theory for AB scattering

At fixed overall impact parameter b the AB amplitude $\mathcal{A}(Y, b)$ can be presented as an exponential of its connected part:

$$\mathcal{A}(Y, b) = 2is \left(1 - e^{-T(Y, b)}\right) \quad (1)$$

The dimensionless T is an integral over two impact parameters b_A and b_B of the collision point relative to the centers of the nuclei A and B:

$$T(Y, b) = \int d^2b_A d^2b_B \delta^2(b - b_A + b_B) T(Y, b_A, b_B) \quad (2)$$

As mentioned in the Introduction, in the perturbative QCD with $N_c \rightarrow \infty$ the amplitude $-T(Y, b_A, b_B)$ is given by a sum of all connected tree diagrams constructed of BFKL pomerons and the triple pomeron vertex. More concretely, in these diagrams a line ("propagator") connecting two points y_1, r_1 and y_2, r_2 corresponds to one half of the forward BFKL Green function [11]:

$$G(y_1 - y_2, r_1, r_2) = \frac{r_1 r_2}{32\pi^2} \theta(y_1 - y_2) \sum_{n=-\infty}^{+\infty} e^{in(\phi_1 - \phi_2)} \int \frac{d\nu e^{(y_1 - y_2)\omega(\nu)} (r_1/r_2)^{-2i\nu}}{\left(\nu^2 + \frac{(n-1)^2}{4}\right) \left(\nu^2 + \frac{(n+1)^2}{4}\right)}, \quad (3)$$

where $\phi_{1,2}$ are the azimuthal angles and

$$\omega(\nu) = \frac{\alpha_s N_c}{\pi} (\psi(1) - \text{Re}\psi(1/2 + i\nu)) \quad (4)$$

are the BFKL levels. Due to the azimuthal symmetry of the projectile and target colour densities one may retain only the term with zero orbital momenta $n = 0$ in (3).

The interaction between the pomerons is realized via the triple pomeron vertex. It is non-local and not symmetric in the incoming and outgoing pomerons. Its form for the splitting of a pomeron into two was established in [2,12,13]. At $N_c \rightarrow \infty$ for the transition $1 \rightarrow 2 + 3$ the three BFKL Green functions are connected by it as follows (see Fig. 1a)

$$\frac{4\alpha_s^2 N_c}{\pi} \int \frac{d^2r_1 d^2r_2 d^2r_3}{r_1^2 r_2^2 r_3^2} \delta^2(r_1 + r_2 + r_3) G(y'_1 - y, r'_1, r_1) \nabla_1^4 r_1^4 G(y - y'_2, r_2, r'_2) G(y - y'_3, r_3, r'_3) \quad (5)$$

Here it is assumed that the operator ∇_1 acts on the left. The form of the vertex for the fusion of two pomerons into one is actually not known. However, the symmetry between target and projectile prompts us to assume that for the inverse process $2 + 3 \rightarrow 1$ the BFKL functions are to be joined as (Fig. 1b)

$$\frac{4\alpha_s^2 N_c}{\pi} \int \frac{d^2r_1 d^2r_2 d^2r_3}{r_1^2 r_2^2 r_3^2} \delta^2(r_1 + r_2 + r_3) G(y'_2 - y, r'_2, r_2) G(y'_3 - y, r'_3, r_3) \nabla_1^4 r_1^4 G(y - y_1, r_1, r'_1) \quad (6)$$

Finally we have to describe the interaction of the pomerons with the two nuclei. The BFKL Green functions corresponding to the external legs of the diagrams are to be integrated

with the colour density of each nucleus. We take the target nucleus at rest, that is, at rapidity zero. Then each outgoing external BFKL Green function is to be transformed into

$$g^2 AT_A(b_A) \int d^2 r' G(y, r, r') \rho_N(r') \equiv \int dy' d^2 r' G(y - y', r, r') \tau_A(y', r') \quad (7)$$

where ρ_N is the colour density of the nucleon, T_A is the profile function of the nucleus A and we define

$$\tau_A(y, r) = g^2 AT_A(b_A) \rho_N(r) \delta(y) \quad (8)$$

(with dependence on b_A implicit). Similarly each ingoing BFKL external Green function is transformed into

$$\int dy' d^2 r' G(y' - y, r', r) \tau_B(y', r') \quad (9)$$

where

$$\tau_B(y, r) = g^2 BT_B(b_B) \rho_N(r) \delta(y - Y) \quad (10)$$

To find the amplitude one has to sum over all connected diagrams with M ingoing and N outgoing lines, corresponding to M interactions with the projectile and N interactions with the target, divided by $M!N!$.

It is trivial to see that this sum exactly corresponds to the sum of tree diagrams generated by an effective quantum theory of two pomeron fields $\Phi(y, r)$ and $\Phi^\dagger(y, r)$ with action

$$S = S_0 + S_I + S_E \quad (11)$$

consisting of three terms, which correspond to free pomerons, their mutual interaction and their interaction with external sources (nuclei) respectively.

To give the correct propagators S_0 has to be chosen as

$$S_0 = 2 \int dy_1 d^2 r_1 dy_2 d^2 r_2 \Phi(y_1, r_1) G^{-1}(y_1 - y_2, r_1, r_2) \Phi^\dagger(y_2, r_2) \equiv 2 \langle \Phi | G^{-1} | \Phi^\dagger \rangle \quad (12)$$

where $\langle | \rangle$ means the integration over y, r . Note that the sign of S_0 corresponds to the substitution of the conventionally defined field variables Φ and Φ^\dagger :

$$\Phi \rightarrow i\Phi, \quad \Phi^\dagger \rightarrow i\Phi^\dagger \quad (13)$$

which allows to make all terms of the action real.

According to (5), (6) the interaction term S_I is local in rapidity

$$S_I = \frac{4\alpha_s^2 N_c}{\pi} \int dy \int \frac{d^2 r_1 d^2 r_2 d^2 r_3}{r_1^2 r_2^2 r_3^2} \delta^2(r_1 + r_2 + r_3) \left[\nabla_1^4 r_1^4 \Phi^\dagger(y, r_1) \Phi(y, r_2) \Phi(y, r_3) + c.c. \right] \quad (14)$$

The overall sign combines the initial factor i and i^3 from the substitution (13).

Finally the interaction with the nuclei is local both in rapidity and coordinates:

$$S_E = - \int dy d^2 r \left[\Phi(y, r) \tau_A(y, r) + \Phi^\dagger(y, r) \tau_B(y, r) \right] \quad (15)$$

The minus sign comes from the initial i and the substitution (13).

The amplitude $T(Y, b_A, b_B)$ is then expressed through a functional integral

$$Z = \int D\Phi D\Phi^\dagger e^{S/\mu^2} \quad (16)$$

where μ is an arbitrary mass scale necessary to adjust the dimensions of various parts of the action. Keeping only the connected diagrams one finds

$$T(Y, b_A, b_b) = -\mu^2 \ln \frac{Z}{Z_0} \quad (17)$$

where Z_0 is the value of Z for $S_E = 0$. Functional integral Z is to be calculated in the classical approximation to retain only the tree diagrams. This gives

$$T(Y, b_A, b_B) = -S_E\{\Phi, \Phi^\dagger\} = \int d^2r \left[\Phi(0, r) \hat{\tau}_A(r) + \Phi^\dagger(Y, r) \hat{\tau}_B(r) \right] \quad (18)$$

where Φ and Φ^\dagger are the solutions of the classical equation of motion and $\hat{\tau}$'s are (8) and (10) with the δ functions of rapidity dropped. We see that the result is independent of the scale μ , as it should be.

3 Equations of motion

Before writing out the classical equation of motion, we transform the functional integral (16) to new variables in which the non-locality of the Lagrangian becomes substantially reduced. We put

$$\Phi(y, r) = r^2 \phi(y, r), \quad \Phi^\dagger(y, r) = r^2 \phi^\dagger(r, y) \quad (19)$$

In these variables the interaction term becomes

$$S_I = \frac{4\alpha_s^2 N_c}{\pi} \int dy \int d^2r_1 d^2r_2 d^2r_3 \delta^2(r_1 + r_2 + r_3) \left[K_1 \phi^\dagger(y, r_1) \phi(y, r_2) \phi(y, r_3) + c.c. \right] \quad (20)$$

where (dimensionless) operator K has the form

$$K = r^2 \nabla_r^4 r^2 \quad (21)$$

Now we transform (20) to the momentum space to obtain

$$S_I = \frac{4\alpha_s^2 N_c}{\pi} \int dy \int \frac{d^2q}{(2\pi)^2} \left[K \phi^\dagger(y, q) \phi(y, q) \phi(y, q) + c.c. \right] \quad (22)$$

with operator K local in the momentum space

$$K = \nabla_q^2 q^4 \nabla_q^2 \quad (23)$$

As we observe, the interaction has become local in the momentum space.

Now we turn to the free part S_0 . In new variables it takes the form

$$S_0 = 2 \langle \phi | r^2 G^{-1} r^2 | \phi^\dagger \rangle \quad (24)$$

It was shown in [6] that

$$r_1^2 \nabla_1^4 G(y, r_1, r_2) = g(y, r_1, r_2) r_2^2 \quad (25)$$

where g is the Green function of the BFKL equation for the so-called semi-amputated wave function:

$$\left(\frac{\partial}{\partial y} + H_1 \right) g(y, r_1, r_2) = \delta(y) \delta^2(r_1 - r_2) \quad (26)$$

Here H_1 is the BFKL Hamiltonian [11] acting on r_1 . We rewrite (26) in the operatorial form

$$K r^{-2} G r^{-2} = \left(\frac{\partial}{\partial y} + H \right)^{-1} \quad (27)$$

wherefrom

$$r^2 G^{-1} r^2 K^{-1} = \frac{\partial}{\partial y} + H \quad (28)$$

and finally

$$r^2 G^{-1} r^2 = \left(\frac{\partial}{\partial y} + H \right) K \quad (29)$$

Since both $G(y, r_1, r_2)$ and $g(y, r_1, r_2)$ are symmetric in r_1, r_2 we also find in the same manner

$$r^2 G^{-1} r^2 = K \left(\frac{\partial}{\partial y} + H \right) \quad (30)$$

so that K commutes with H . Using (29) and (30) in (24) we see that the free part has become local in rapidity and can be expressed via the BFKL Hamiltonian H :

$$S_0 = 2 \langle \phi | K \left(\frac{\partial}{\partial y} + H \right) | \phi^\dagger \rangle \quad (31)$$

This part remains non-local both in the coordinate and momentum spaces due to the non-locality of H .

The interaction with the nucleus part in the new variables takes the form

$$S_E = -\langle w_A | \phi \rangle - \langle \phi^\dagger | w_B \rangle \quad (32)$$

where, in the coordinate space,

$$w_{A,B}(y, r) = r^2 \tau_{A,B}(y, r) \quad (33)$$

Now, with the action nearly completely local (except for the Hamiltonian term) we can write out the equation of motion. We find

$$\frac{\delta S}{\delta \phi(y, q)} = 2K \left(\frac{\partial}{\partial y} + H \right) \phi^\dagger(y, q) + \frac{4\alpha_s^2 N_c}{\pi} \left(K \phi^{\dagger 2}(y, q) + 2\phi(y, q) K \phi^\dagger(y, q) \right) - w_A(y, q) = 0 \quad (34)$$

and

$$\frac{\delta S}{\delta \phi^\dagger(y, q)} = 2K \left(-\frac{\partial}{\partial y} + H \right) \phi(y, q) + \frac{4\alpha_s^2 N_c}{\pi} \left(K \phi^2(y, q) + 2\phi^\dagger(y, q) K \phi(y, q) \right) - w_B(y, q) = 0 \quad (35)$$

Applying operator $(1/2)K^{-1}$ from the left we find our final equations of motion

$$\left(\frac{\partial}{\partial y} + H \right) \phi^\dagger(y, q) + \frac{2\alpha_s^2 N_c}{\pi} \left(\phi^{\dagger 2}(y, q) + 2K^{-1}[\phi(y, q) K \phi^\dagger(y, q)] \right) - \frac{1}{2}K^{-1}w_A(y, q) = 0 \quad (36)$$

and

$$\left(-\frac{\partial}{\partial y} + H \right) \phi(y, q) + \frac{2\alpha_s^2 N_c}{\pi} \left(\phi^2(y, q) + 2K^{-1}[\phi^\dagger(y, q) K \phi(y, q)] \right) - \frac{1}{2}K^{-1}w_B(y, q) = 0 \quad (37)$$

As we see the resulting equations are rather complicated, since they involve nonlocal terms, bilinear in ϕ and ϕ^\dagger , which interconnect the two equations. Summing fan diagrams in the hA case in fact leads to the the same equations, in which however $w_B = 0$. Then one immediately finds that $\phi = 0$ identically, which converts the first equation into

$$\left(\frac{\partial}{\partial y} + H \right) \phi^\dagger(y, q) + \frac{2\alpha_s^2 N_c}{\pi} \phi^{\dagger 2}(y, q) - \frac{1}{2}K^{-1}w_A(y, q) = 0 \quad (38)$$

This local equation is just the one studied in [4-6].

To conclude this section we present the non-local terms in Eqs. (36) and (37) in a more explicit way. To this end we calculate the kernel of the operator K^{-1} in the momentum space. We have in the coordinate space

$$K^{-1} = r^{-2} \nabla_r^{-4} r^{-2} \quad (39)$$

Using the identity [6]

$$\nabla_1^4 G(0, r_1, r_2) = \delta^2(r_1 - r_2) \quad (40)$$

we can write the kernel of K^{-1} in the coordinate space as

$$K^{-1}(r_1, r_2) = r_1^{-2} G(0, r_1, r_2) r_2^{-2} \quad (41)$$

Fourier transforming (41) and using (3) we find the kernel in the momentum space:

$$K^{-1}(q_1, q_2) = \int \frac{d^2 r_1 d^2 r_2}{r_1^2 r_2^2} e^{iq_2 r_2 - iq_1 r_1} G(0, r_1, r_2) = \frac{1}{8} \int \frac{d\nu}{(\nu^2 + 1/4)^2} I(\nu, q_1) I^*(\nu, q_2) \quad (42)$$

where

$$I(\nu, q) = \int_0^\infty dr r^{-2i\nu} J_0(qr) = 2^{-2i\nu} q^{-1+2i\nu} \frac{\Gamma(1/2 - i\nu)}{\Gamma(1/2 + i\nu)} \quad (43)$$

Doing the integral over ν we finally find

$$K^{-1}(q_1, q_2) = \frac{\pi}{2} \frac{1}{q_{>}^2} \left(\ln \frac{q_{>}}{q_{<}} + 1 \right) \quad (44)$$

where $q_{>(<)} = \max(\min)\{q_1, q_2\}$.

Using (44) we can rewrite the nonlocal term in Eq. (36) as

$$4\alpha_s^2 N_c \int \frac{d^2 q_1}{(2\pi)^2 q_{>}^2} \left(\ln \frac{q_{>}}{q_{<}} + 1 \right) \phi(y, q_1) \nabla_1^2 q_1^4 \nabla_1^2 \phi^\dagger(y, q_1) \quad (45)$$

where $q_{>(<)} = \max(\min)\{q, q_1\}$. The nonlocal term in Eq. (37) is obtained by complex conjugation.

4 The total cross-section

The obtained equations which determine the classical fields ϕ and ϕ^\dagger are very difficult to solve even numerically. The trouble lies not so in their explicit non-locality, but in the appearance of two different sources at two different rapidities. Due to conditions $\phi = 0$ for $y > Y$ and $\phi^\dagger = 0$ for $y < 0$ and the δ -like dependence of the sources on rapidities, one can drop the sources in Eq. (36) and (37) substituting them by conditions

$$\phi^\dagger(y, q)_{y=0} = K^{-1} \hat{w}_A(q), \quad \phi(y, q)_{y=Y} = K^{-1} \hat{w}_B(q) \quad (46)$$

In the hA case one has only the first of these conditions, which converts Eq. (36) into an evolution equation in rapidity, relatively easily solved by conventional methods. As mentioned the non-local term is zero in this case, but its presence would only slightly complicate the solution. After all the BFKL Hamiltonian is also non-local (although linear).

For the nucleus-nucleus scattering we have to solve homogeneous Eqs (36) and (37) with both conditions (46) imposed upon the solution. The Cauchy problem is thus transformed into an essentially more difficult boundary problem. A possible method of the solution is to transform Eqs. (36) and (37) into a system of two non-linear integral equations in combined

rapidity-momentum space, which one may try to solve by iterations. Our experience in the hA problem shows that for the solution to have a reasonable precision one requires at least 800 points in the momentum and 400 points for 5 units of rapidity. Thus to find the amplitude for say $Y = 15$ one has to perform $1200 \times 800^3 \sim 10^{10}$ operations per iteration. On top of that the convergence properties of the iteration procedure is unknown.

Here we shall not attempt at solving Eqs. (36) and (37) with any reasonable degree of precision at all values of rapidity and momentum. Instead we shall again use our experience with the case of hA scattering (fan diagrams), where at any fixed momentum and $y \rightarrow \infty$ the solution $\phi^\dagger(y, q)$ acquires a simple form, independent of the target properties

$$\phi^\dagger(y, q)_{y \rightarrow \infty} = \frac{2\pi}{g^2} \ln \frac{Q(y)}{q} \quad (47)$$

with $\ln Q(y) \simeq 2.34(\alpha_s N_c / \pi)y$. Note that (47) is not the solution at all y and q . In particular (47) is not valid at $q \sim Q$, which is just the region which determines the gluon density. However (47) is sufficient to establish that the hA scattering cross-section tends to its geometric limit at high y [7].

Our guess is that also in the nucleus-nucleus case function $\phi^\dagger(y, q)$ acquires the form (47) at large rapidities $y \sim Y$ and $\phi(y, q)$ acquires the same form with $y \rightarrow Y - y$. To support this behaviour we are going to demonstrate that in these limits the non-local terms in Eqs. (36) and (37) can be neglected, so that the equations decouple and become similar to the hA case.

Actually the demonstration is quite simple. Take Eq. (36) at large y and put the conjectured asymptotics (47) into it. According to (45) the mixing non-local term will then be given by

$$\alpha_s N_c \int \frac{d^2 q_1}{(2\pi)^2 q_1^2} \left(\ln \frac{q_>}{q_<} + 1 \right) \phi(y, q_1) \nabla_1^2 q_1^4 \nabla_1^2 \ln \frac{Q(y)}{q_1} \quad (48)$$

Note that $\phi(y, q_1)$ enters at large y and small $Y - y$. Its exact form is unknown but we can safely assume that it rapidly falls with q_1 similar to the inhomogeneous term $K^{-1} w_B$ from which it is separated by a relatively small distance in rapidity. Action of the operator $K = \nabla^2 q^4 \nabla^2$ on the asymptotic form of ϕ^\dagger however gives zero. In fact

$$\nabla_1^2 \ln \frac{Q(y)}{q_1} = -2\pi \delta^2(q_1)$$

Subsequent integration over q_1 gives zero at any finite q due to factor q_1^4 . Thus the non-local term is zero in Eq. (36) at $y \sim Y \rightarrow \infty$. Therefore the equation acquires the same form as for hA scattering (which implies that fan diagrams going from top to bottom dominate). This means that the asymptotical behaviour (47) is indeed true. The same result is found for the non-local term in Eq. (37) at small y and $Y - y \rightarrow \infty$ assuming the asymptotic form (47) for $\phi(Y - y, q)$. Its meaning is that fan diagrams going from bottom to top dominate in this limit.

Functions $\Phi(y, r)$ and $\Phi^\dagger(y, r)$ which actually determine the amplitude according to (18) are related to $\phi(y, q)$ and $\phi^\dagger(y, q)$ by

$$\Phi(y, r) = - \int \frac{d^2 q}{(2\pi)^2} e^{iqr} \nabla_q^2 \phi(y, q) \quad (49)$$

and similarly for the conjugated function. Using the asymptotical expression (47) we then get at high Y

$$\Phi(0, r) = \frac{1}{g^2} \theta(R_B - b_B), \quad \Phi^\dagger(Y, r) = \frac{1}{g^2} \theta(R_A - b_A) \quad (50)$$

The two θ functions appear because according to Eqs. (36) and (37) $\phi = 0$ ($\phi^\dagger = 0$) when $w_B = 0$ ($w_B = 0$), that is for $b_B > R_B$ ($b_A > R_A$).

Putting (50) in (18) we obtain the connected part of the amplitude at $Y \gg 1$ as

$$T(Y, b_A, b_B) = AT_A(b_A)\theta(R_B - b_B) + T_B(b_B)\theta(R_A - b_A) \quad (51)$$

It results independent of Y . After the integration over b_B and b_B we find

$$T(Y, b) = \int d^2b_A d^2b_B \delta^2(b - b_A + b_B) \theta(R_A - b_A) \theta(R_B - b_B) [AT_A(b_A) + BT_B(b_B)] \quad (52)$$

According to (1) the total AB cross-section is given by

$$\sigma^{tot}(Y) = 2 \int d^2b \left(1 - e^{-T(Y, b)}\right) \quad (53)$$

From (52) and (53) one concludes that at large Y the cross-section does not depend on Y . It saturates at a value which is purely geometrical and for $A \gg 1$ or/and $B \gg 1$ approaches the black disk limit in the overlap area.

5 Conclusions

We have derived a pair of equations which describe the nucleus-nucleus scattering in the perturbative QCD with a large number of colours (or, alternatively in the quasi-classical limit, or, in the limit $A, B \rightarrow \infty$). The equations contain mixing terms which are both non-linear and non-local. In contrast to the hA case the equations are to be solved with given boundary conditions at rapidities both of the projectile and target, which complicates the solution enormously.

However the asymptotical form of the solution at fixed momentum and large rapidities is shown to be the same as for the hA case. This allows to demonstrate that at large rapidities the total AB cross-section becomes independent of energy and given by purely geometric considerations. At large A or/and B it corresponds to the scattering on the black disc in the overlap area.

Going to particle production in AB collisions, the situation at central rapidities seems to be rather simple. The inclusive cross-section will be described by diagrams like shown in Fig. 2, with the target and projectile parts joined by a single pomeron, from which the observed particle is emitted. Evidently this contribution is just a convolution of the production vertex with two gluon densities of the projectile and target, each one corresponding to fan diagrams and found in [6]. At rapidity distances from the target or projectile $\delta y \sim 1/\Delta$ where Δ is the pomeron intercept the problem does not look so simple, since the AGK rules are rather complicated in this region (see e. g. [14]) and the usual cancellation of all diagrams except of the structure shown in Fig. 2 is not at all obvious. We leave this problem for future studies.

6 References

1. A.Mueller, Nucl. Phys., **B415** (1994) 373.
2. A.Mueller and B.Patel, Nucl. Phys., **B425** (1994) 471.
3. M.A.Braun and G.P.Vacca, Eur. Phys. J **C6** (1999) 147.
4. I.Balitsky, hep-ph/9706411; Nucl. Phys. **B463** (1996) 99.
5. Yu. Kovchegov, Phys. Rev **D60** (1999) 034008.
6. M.Braun, preprint LU TP 00-06 (hep-ph/0001268)
7. Yu. Kovchegov, preprint CERN-TH/99-166 (hep-ph/9905214).

- 8 .E.Levin and K.Tuchin, preprint DESY 99-108, TAUP 2592-99 (hep-ph/9908317).
9. A.Schwimmer, Nucl. Phys. B94 (1975)445.
10. D.Amati, L.Caneshi and R.Jengo, Nucl. Phys. **B101** (1975) 397.
11. L.N.Lipatov in: "Perturbative QCD", Ed. A.H.Mueller, World Sci., Singapore (1989) 411.
12. J.Bartels and M.Wuesthoff, Z.Phys., **C66** (1995) 157.
13. M.A.Braun, Eur. Phys. J **C6** (1999) 321.
14. M.Ciafaloni *et al.*, Nucl. Phys. **B98** (1975) 493.

7 Figure captions

Fig. 1. The triple pomeron vertex for the splitting of a pomeron into two (a) and fusion of two pomerons into one (b).

Fig. 2. The generic diagram for the inclusive particle production in the central region in AB collisions

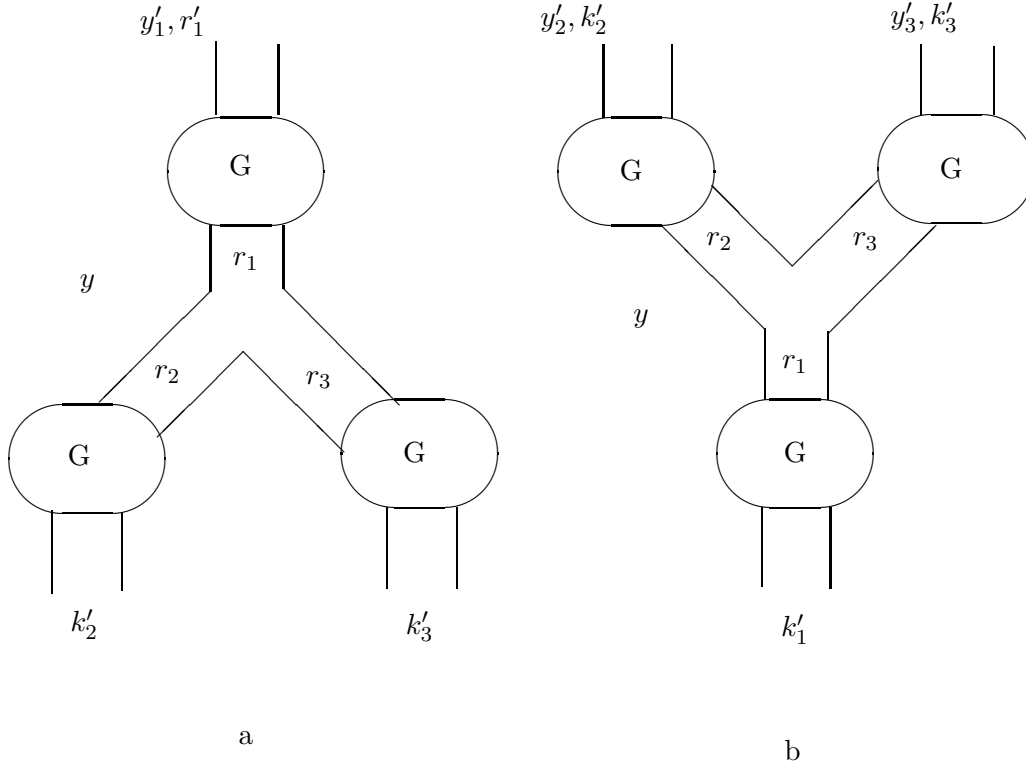


Fig. 1

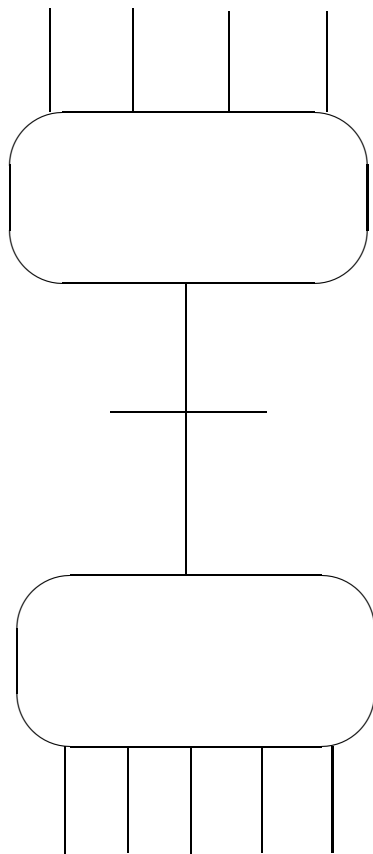


Fig. 2